Molecular Biology of the Cell
Vol. 15, 2943–2953, June 2004

Vascular Endothelial-Cadherin Regulates Cytoskeletal Tension, Cell Spreading, and Focal Adhesions by Stimulating RhoA[D]

Celeste M. Nelson, Dana M. Pirone, John L. Tan, and Christopher S. Chen*

Departments of Biomedical Engineering and Oncology, Johns Hopkins School of Medicine, Baltimore, Maryland 21205

Submitted October 17, 2003; Revised March 22, 2004; Accepted March 22, 2004
Monitoring Editor: Martin A. Schwartz

Changes in vascular endothelial (VE)-cadherin–mediated cell-cell adhesion and integrin-mediated cell-matrix adhesion coordinate to affect the physical and mechanical rearrangements of the endothelium, although the mechanisms for such cross talk remain undefined. Herein, we describe the regulation of focal adhesion formation and cytoskeletal tension by intercellular VE-cadherin engagement, and the molecular mechanism by which this occurs. Increasing the density of endothelial cells to increase cell-cell contact decreased focal adhesions by decreasing cell spreading. This contact inhibition of cell spreading was blocked by disrupting VE-cadherin engagement with an adenovirus encoding dominant negative VE-cadherin. When changes in cell spreading were prevented by culturing cells on a micropatterned substrate, VE-cadherin–mediated cell-cell contact paradoxically increased focal adhesion formation. We show that VE-cadherin engagement mediates each of these effects by inducing both a transient and sustained activation of RhoA. Both the increase and decrease in cell-matrix adhesion were blocked by disrupting intracellular tension and signaling through the Rho-ROCK pathway. In all, these findings demonstrate that VE-cadherin signals through RhoA and the actin cytoskeleton to cross talk with cell-matrix adhesion and thereby define a novel pathway by which cell-cell contact alters the global mechanical and functional state of cells.

INTRODUCTION

Coordinated changes between cell adhesion to the extracellular matrix (ECM) and to neighboring cells are crucial for the many physical transformations that cells must undergo during development, tissue homeostasis, and wound healing. In the endothelium, where a single layer of cells separates tissues from their blood supply, the concerted regulation of cell-cell and cell-ECM adhesion drives rapid changes in cell shape and vascular architecture essential to vascular remodeling in both normal and disease processes (Vestweber, 2000; Dudek and Garcia, 2001). Dynamic changes in cell-cell and cell-matrix adhesion and mechanical forces are responsible for regulating vascular permeability, and agents that alter permeability invariably affect both types of adhesion complexes (Dudek and Garcia, 2001). During blood vessel sprouting and migration in angiogenesis, endothelial cells must disassemble and reform their cell-cell and cell-ECM contacts in synchrony to generate appropriate structures. These two adhesion systems each regulate their functional effects through both biochemical and mechanical signals.

Article published online ahead of print. Mol. Biol. Cell 10.1091/mbc.E03–10–0745. Article and publication date are available at www.molbiolcell.org/cgi/doi/10.1091/mbc.E03–10–0745.

[D] Online version of this article contains supporting material. Online version is available at www.molbiolcell.org.

* Corresponding author. E-mail address: cchen@bme.jhu.edu.

Abbreviations used: EMT, epithelial-mesenchymal transition; FA, focal adhesion; ROCK, Rho kinase; VE-cadherin, vascular endothelial-cadherin.

Changes in integrin binding to ECM not only alter signals that regulate cell proliferation, migration, and survival (Assoian and Schwartz, 2001; Hood and Cheresh, 2002; Stupack and Cheresh, 2002) but also modulate cell mechanics by affecting focal adhesion (FA) maturation, adhesion strength, cytoskeletal contractility, and cell shape (Geiger and Bershadsky, 2002; Juliano, 2002). Likewise, changes in the engagement of vascular endothelial (VE)-cadherin, the principal junctional molecule in endothelial cells (Dejana *et al*., 1999), alter both biochemical pathways, such as vascular endothelial growth factor (VEGF) and cell survival signaling (Carmeliet *et al*., 1999), as well as mechanical states by altering cytoskeletal organization and the local transfer of mechanical stress (Shay-Salit *et al*., 2002). Although the biochemical and mechanical consequences of integrin- and cadherin-mediated adhesion each have been described, how these adhesions cross talk and cooperate is less well understood.

Although studies have reported that cell-cell cohesivity through cadherins competitively decreases cell-substratum adhesivity, a process known as contact inhibition of cell adhesion and spreading (Yap and Manley, 1993; Ryan *et al*., 2001), an explanation for the underlying mechanism remains elusive. Cadherin engagement between cells leads to the formation of adherens junctions, the cytoplasmic face of which consists of an adhesion plaque containing many of the same structural proteins as are found in FAs (Pokutta and Weis, 2002). VE-cadherin–mediated contact could thus affect integrin-mediated adhesion indirectly by competing for a limited pool of these shared molecules (Levenberg *et al*., 1998). Cadherin-mediated adhesion also directly initiates both mechanical and biochemical signals known to affect FA formation. First, mechanical stress exerted at cadherin cell

junctions can be transmitted through the actin cytoskeleton directly to FAs (Davies *et al*., 1997; Ko *et al*., 2001; Shay-Salit *et al*., 2002). Because FAs are sensitive to such forces, changes in VE-cadherin binding likely alter FA formation mechanically (Geiger and Bershadsky, 2001). Second, VE-cadherin engagement activates numerous biochemical pathways that have been shown to affect cell shape, cytoskeletal mechanics, and cell-ECM adhesion, including Rac and Cdc42, members of the Rho family of small GTPases (Carmeliet *et al*., 1999; Etienne-Manneville and Hall, 2002; Juliano, 2002; Lampugnani *et al*., 2002; Kouklis *et al*., 2003). Yet, despite the logical existence and biological ramifications of cross talk between these adhesion systems, previous attempts to demonstrate specifically the effects of cell-cell contact on cell-ECM adhesion have remained controversial.

A principal difficulty in studying cross talk has been that the traditional methods of varying cadherin-mediated adhesion also directly affect cell-ECM adhesion. Reducing extracellular calcium in the calcium switch assay not only destabilizes cadherins but also alters integrin-mediated adhesion, cell spreading, and myosin-mediated contractility (Hodivala and Watt, 1994). In comparisons of confluent monolayers to sparse cultures, one not only observes changes in cell-cell contact, but increasing cell density causes cells to crowd for space on the underlying substratum. These changes in cell shape may themselves alter cell-ECM adhesion (Chen *et al*., 2003), again making it difficult to isolate and interpret the effects of cell-cell contact. Our laboratory has recently developed microfabrication-based strategies to overcome these experimental hurdles (Nelson and Chen, 2002, 2003). By controlling the placement and organization of cells on micropatterned substrates, we have independently manipulated cell-cell and cell-ECM contact to study their relative roles in the regulation of proliferation.

Here, we investigated the mechanism by which VE-cadherin engagement specifically alters cell-ECM adhesion in endothelial cells. We show that VE-cadherin induces both a transient and sustained activation of RhoA resulting in increased intracellular tension and decreased cell spreading, and this activation can either strengthen or disassemble FAs, depending on the microenvironment. These data provide one molecular description of the coordination of mechanochemical signals between cell-cell and cell-ECM adhesion that drive the complex transitions essential to multicellular reorganization.

MATERIALS AND METHODS

Materials

The following reagents were purchased from the given suppliers: human fibronectin (Collaborative Research, Bedford, MA); bovine serum albumin (BSA; Serologicals, Norcross, GA); 2,3-butanedione 2-monoxime (BDM; Calbiochem, San Diego); Y-27632 (Calbiochem); anti-FAK clone 2A7 (Upstate Biotechnology, Lake Placid, NY); anti-FAK clone 77 (BD Transduction Laboratories, Lexington, KY); anti-vinculin clone hVin-1 (Sigma-Aldrich, St. Louis, MO); anti-talin clone 8D4 (Sigma-Aldrich); anti-phosphotyrosine clone 4G10 (Upstate Biotechnology); tetramethylrhodamine B isothiocyanate (TRITC)-conjugated phalloidin (Sigma-Aldrich); polyclonal rabbit anti-VE-cadherin (Alexis, Läufelfingen, Switzerland); anti-β-catenin clone E-5 (Santa Cruz Biotechnology, Santa Cruz, CA); anti-connexin 43 (Chemicon International, Temecula, CA); anti-platelet-endothelial cell adhesion molecule-1 (PECAM-1) (Santa Cruz Biotechnology); polyclonal rabbit anti-RhoA (Santa Cruz Biotechnology); and anti-p120-catenin clone 98 (BD Transduction Laboratories). Stock solutions (100×) of BDM and Y-27632 were dissolved per manufacturers' instructions in methanol and water, respectively.

Cell Culture

Bovine pulmonary artery endothelial cells (VEC Technologies, Rensselaer, NY; passages 6–12) were maintained in low glucose DMEM supplemented with 5% calf serum, 100 U/ml penicillin, and 100 μg/ml streptomycin (all from Invitrogen, Carlsbad, CA). Cells were synchronized at confluence before plating on substrates. Antagonists were added to cells in full culture medium at 2 h after plating, and maintained in the medium until cells were fixed at 24 h. Human carcinoma A431D (null) and A431D-VE (VE^+) cells were a generous gift from K. Johnson (University of Nebraska, Lincoln, NE), and were cultured in high glucose DMEM supplemented with 10% fetal bovine serum, 100 U/ml penicillin, and 100 μg/ml streptomycin, with VE^+ or without (null) 1 μg/ml puromycin (AG Scientific, San Diego, CA).

Density Experiments

Glass coverslips or tissue culture dishes were coated with a 25 μg/ml solution of fibronectin in phosphate-buffered saline (PBS) for 2 h, washed twice in PBS, and then blocked in 1% BSA in PBS for 2 h. G_0-synchronized cells were plated on washed substrates in full culture media. To obtain changes in cell spreading, cells fixed and stained at 24 h after plating with TRITC-conjugated phalloidin were photographed with a Spot charge-coupled device camera (Diagnostic Instruments, Sterling Heights, NY), and mean cell area was determined by outlining fluorescence images of the cells with the Spot software; cells had not yet entered mitosis at this time point (Nelson and Chen, 2003). To ensure an accurate representation of the spreading of the population of cells, 100 randomly chosen cells were analyzed per experiment, regardless of degree of contact with neighboring cells, and two independent experiments were conducted per condition.

Fabrication of Substrates with Microwells

Substrates composed of bowtie-shaped microwells of agarose on glass (750 μm^2/half bowtie) were fabricated as described previously (Nelson and Chen, 2002). Briefly, masters of patterned SU-8 photoresist (MicroChem, Newton, MA) were prepared by conventional photolithography. Stamps of poly(dimethylsiloxane) were made by treating the masters with a vapor of (tridecafluoro-1,1,2,2-tetrahydrooctyl)-1-trichlorosilane (United Chemical Technologies, Bristol, PA) for 30 min and then curing Sylgard 184 (Dow-Corning, Midland, MI) for >1 h against the silanized master. A solution of 0.6% agarose/40% ethanol in water was perfused through the channels created by sealing a stamp against a SuperFrost slide (Fisher Scientific, Pittsburgh, PA) and dried under vacuum. Peeling off the stamp unmasked regions of bare glass on the substrate. Substrates were sterilized in ethanol, washed in PBS, and incubated in a 25 μg/ml solution of fibronectin in PBS for 2 h.

Immunofluorescence

Cells were fixed and stained at 24 h after seeding. For the detection of cell-cell adhesion molecules, cells were fixed in 4% paraformaldehyde in PBS, permeabilized in 0.2% Triton X-100 in PBS, washed in 33% goat serum in PBS, incubated in primary antibodies diluted in 33% goat serum in PBS, and visualized with Alexa 488-conjugated secondary antibodies (Molecular Probes, Eugene, OR).

Quantitative Analysis of FAs

For immunofluorescence staining of FA proteins, cells were fixed and processed at 24 h after initial plating. Coverslips were incubated for 1 min in ice-cold cytoskeleton stabilizing buffer [50 mM NaCl, 150 mM sucrose, 3 mM $MgCl_2$, 1 μg/ml aprotinin, 1 μg/ml leupeptin, 1 μg/ml pepstatin, 10 mM piperazine-*N*,*N*′-bis(2-ethanesulfonic acid), pH 6.8], followed by 1 min in ice-cold cytoskeleton stabilizing buffer supplemented with 0.5% Triton X-100 (Plopper and Ingber, 1993). Detergent-extracted cells were fixed in 4% paraformaldehyde in PBS for 5 min, washed with PBS, blocked in goat serum, and incubated with primary antibodies diluted in goat serum in PBS. Primary antibodies were visualized using Alexa 488- and Alexa 594-conjugated goat IgGs (Molecular Probes). Quantitative microscopy of FA proteins was carried out using a Hamamatsu Orca charge-coupled device camera attached to an inverted Nikon TE200 microscope by using a 100×/1.40 numerical aperture oil objective. Images were obtained and processed at room temperature by using IP Lab version 3.0 as follows: Original images of immunostained cells were filtered and binarized to subtract background fluorescence; filtered, binary images were segmented with a threshold of 0.25 μm^2 to quantify the area of individual adhesion sites. Analysis was performed on 100 cells over two independent experiments.

For quantification of FAs by Western blotting, cells were washed twice in cold PBS and then permeabilized for 10 min with ice-cold permeabilization buffer (10 mM HEPES, pH 6.9, 0.1% Triton X-100, 50 mM NaCl, 3 mM $MgCl_2$, 300 mM sucrose, 1 mM EGTA, 1 mM phenylmethylsulfonyl fluoride [PMSF], 1 μg/ml each aprotinin, leupeptin, and pepstatin), followed by a brief rinse with the same buffer (Putnam *et al*., 2003). The remaining detergent-insoluble proteins were solubilized in lysis buffer (25 mM Tris-HCl, pH 7.4, 0.4 M NaCl, 0.5% SDS, 1 mM PMSF, 1 μg/ml each aprotinin, leupeptin, pepstatin) for 5 min. Total cellular protein was obtained by lysing cells directly in lysis buffer after four washes with PBS. Lysates from equal numbers of cells were analyzed by Western blotting.

Western Blotting

Cells were washed twice in PBS and lysed in ice-cold modified radioimmunoprecipitation assay buffer (50 mM Tris-HCl, pH 7.4, 1% NP-40, 0.25% deoxycholate, 150 mM NaCl, 1 mM EDTA, 1 mM PMSF, 1 mM orthovanadate, 1 mM NaF, 1 μg/ml each aprotinin, leupeptin, and pepstatin). Proteins in the lysates were separated by denaturing SDS-PAGE on 7.5% polyacrylamide gels, electroblotted onto nitrocellulose, blocked with 4% BSA in Tris-buffered saline, immunoblotted with specific primary antibodies, and detected using horseradish peroxidase-conjugated secondary antibodies (Amersham Biosciences, Piscataway, NJ) and SuperSignal West Dura (Pierce Chemical, Rockford, IL) as a chemiluminescent substrate. Densitometry analysis was performed using a VersaDoc imaging system with Quantity One software (Bio-Rad, Hercules, CA).

Construction of Recombinant Adenoviruses

Recombinant adenovirus encoding $RhoA^{N19}$ and human VE-cadherin lacking the β-catenin binding domain (VEΔ) were prepared using the AdEasy XL system (Stratagene, La Jolla, CA) per kit instructions. Briefly, the cDNA fragment encoding $RhoA^{N19}$ was mutagenized from pEGFP-WT-RhoA (gift from M. Philips, New York University, New York, NY). The cDNA fragment encoding VEΔ (Navarro *et al.*, 1995; Lampugnani *et al.*, 2002) was polymerase chain reaction amplified from pBluescript-VE-cadherin-EGFP (clone 35–21; gift from S. Shaw and F. Luscinskas, Brigham and Women's Hospital, Boston, MA) by using the following primers: 5′-GAGGCGGCCGCCCACCATGCA-GAGGCTCATGATG-3′ and 5′-GAGCTCGAGCTAATACAGCAGCTCCTC-CCGGGGG-3′. Both fragments were polymerase chain reaction amplified and cloned into the shuttle vector pShuttle-IRES-hrGFP-1. After construction, the shuttle vectors were linearized with *Pme* I and transformed into BJ5183-AD-1 competent cells pretransformed with the pAdEasy-1 adenoviral vector, to generate recombinant adenoviral plasmids, which were purified and transfected into human embryonic kidney 293 cells. Adenoviral infection was monitored by green fluorescent protein (GFP) fluorescence, and adenoviral particles were obtained by cell extraction after 7–10 d. The virus was further amplified and purified by centrifugation on a CsCl gradient. Stocks of 10^9-10^{10} infectious particles/ml were retained and used in subsequent experiments. The virus was titrated by infecting human embryonic kidney 293 cells with serially diluted stocks and counting GFP-expressing cells.

To infect endothelial cells, a solution of recombinant adenovirus was mixed with culture medium, and cells were exposed to the virus with a multiplicity of 10–100 viral particles/cell for 3 h. Cells were then washed, trypsinized, and plated onto substrates. Cells were fixed and analyzed 24 h after plating; under these conditions, >95% of the cells were infected. For the pulldown time courses, cells were exposed to virus for 3 h, washed, and replated 24 h after infection. Cells were analyzed at various time points after replating.

Detection of Active RhoA

Activated RhoA was measured following the method of Ren *et al.*, 1999. Cells were washed twice with ice-cold Tris-buffered saline and scraped in ice-cold lysis buffer (50 mM Tris, pH 7.2, 1% Triton X-100, 0.5% sodium deoxycholate, 0.1% SDS, 500 mM NaCl, 10 mM $MgCl_2$, 10 μg/ml each of leupeptin and aprotinin, and 1 mM PMSF). Cell lysates were centrifuged at 13,000 $\times$ *g* at 4°C for 3 min, and equal volumes of lysates were incubated with glutathione *S*-transferase-rho-binding domain beads (30 μg; Upstate Biotechnology) at 4°C for 45 min. The beads were washed three times with wash buffer (50 mM Tris, pH 7.2, 1% Triton X-100, 150 mM NaCl, 10 mM $MgCl_2$, 10 μg/ml each of leupeptin and aprotinin, and 0.1 mM PMSF) and eluted by boiling in Laemmli sample buffer for 5 min. Bound Rho proteins were detected by Western blotting. The level of RhoA activity (GTP-bound RhoA) in different samples was determined by normalizing the amount of RBD-bound RhoA to the total amount of RhoA in cell lysates.

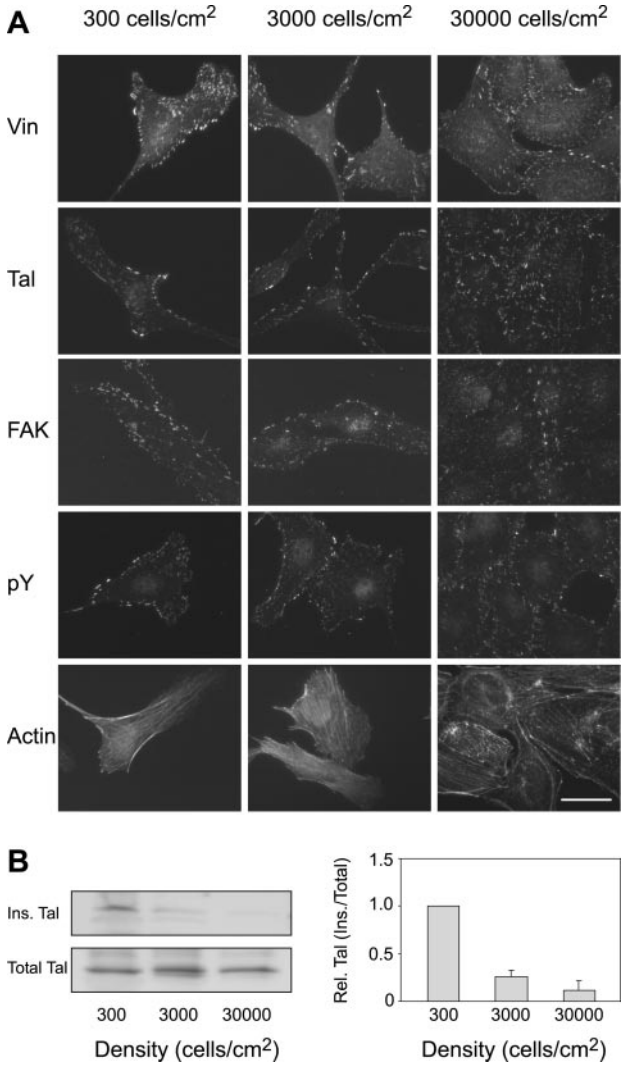

Figure 1. Density modulates FA formation. (A) Fluorescence images of cells seeded at different densities and stained for FA components, vinculin (vin), talin (tal), FAK, and phosphotyrosine (pY), or actin. Bar, 25 μm. (B) Western blot for Triton X-100 insoluble fraction (ins.) and total talin at different seeding densities (left). Graph of relative talin in FA (ins./total) at different seeding densities (right). Error bars indicate SD of three independent experiments.

RESULTS

Cell-Cell Contact Decreases Cell Adhesion to ECM and Cell Spreading

To investigate how cell-cell contact might modulate cell-ECM adhesion in endothelial cells, we first examined the formation of FAs in cells exposed to different degrees of cell-cell adhesion. Bovine pulmonary artery endothelial cells were plated at seeding densities ranging from 300 to 30,000 cells/cm^2 to vary cell-cell contact. After 24 h, cells were fixed and analyzed for FA formation. Endothelial cells plated at low seeding densities (300 cells/cm^2) did not make contact with their neighbors and formed many prominent FAs, as observed by immunofluorescence analysis of vinculin, talin, FAK, and phosphotyrosine (Figure 1A). As seeding density increased, cell-cell contact increased and FAs decreased, consistent with previous reports (Hormia *et al.*, 1985). Quantifying FA formation by Western blot analysis of FA proteins in Triton X-100–insoluble fractions of cell lysates also showed decreased FAs with increased cell-cell contact (Figure 1B). Cells at the highest seeding density had 85% less Triton X-100–insoluble talin than did cells at the lowest seeding density.

Increasing seeding density not only decreased FAs but also seemed to alter the degree of endothelial cell spreading on the fibronectin-coated substrates, as demonstrated by immunofluorescence of actin (Figure 1A). To quantify this effect, the degree of cell spreading and FA formation were measured together on a cell-by-cell basis by calculating projected cell area and the total area and number of FAs per cell based on immunofluorescence staining of vinculin, talin, FAK, and phosphotyrosine (Figure 2, A and B). Cells were plated at a low density as a baseline control to prevent the

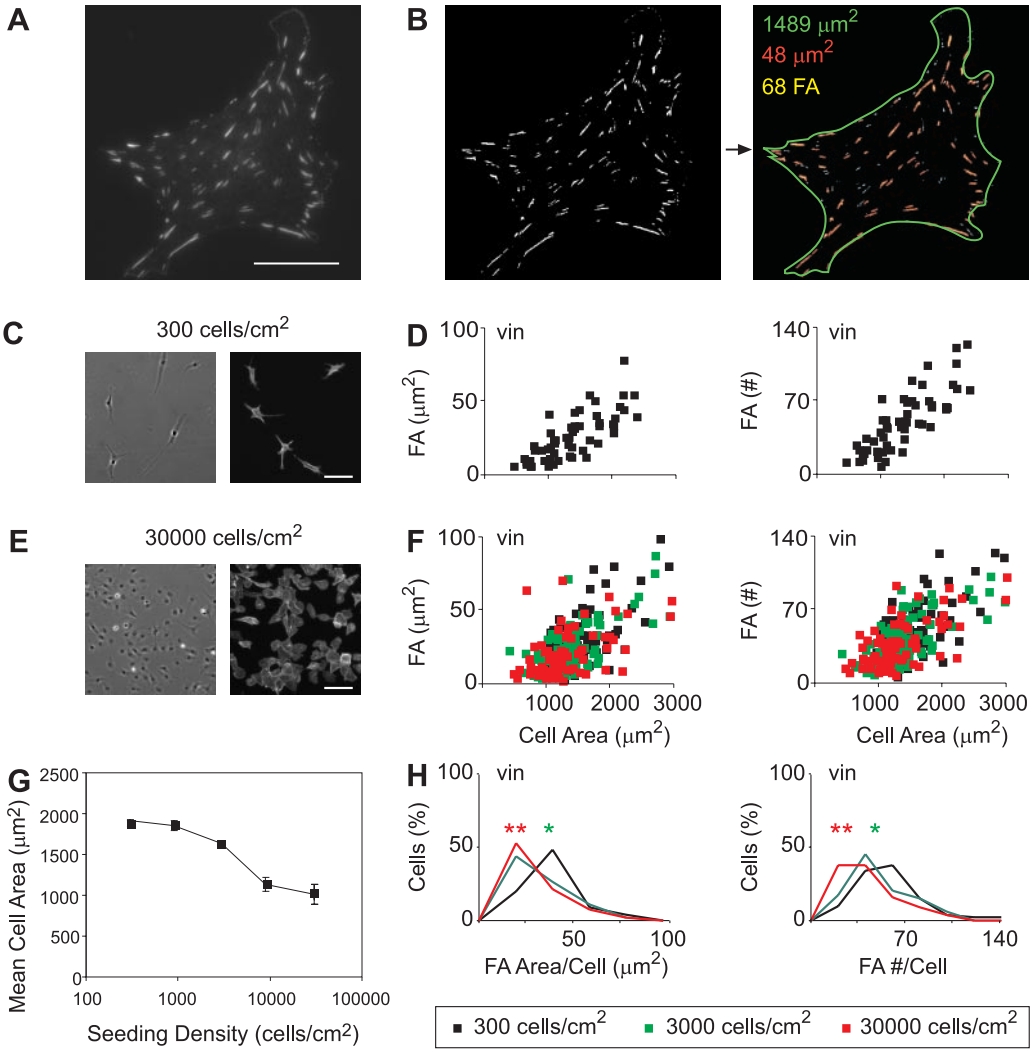

Figure 2. Cell-cell contact decreases cell spreading and FA formation. (A) Fluorescence image of cell stained for vinculin. Bar, 25 μm. (B) Black/white image of vinculin fluorescence of cell in A after processing (left), with cell area (green), FA area (red), and FA number (yellow) indicated for that cell (right). (C) Phase contrast (left) and fluorescence images (right) of cells seeded at 300 cells/cm² and stained with TRITC-conjugated phalloidin. Bar, 200 μm. (D) Dot plots of total FA area (left) and number (right) as a function of cell spreading for cells plated at a low density. (E) Phase contrast (left) and fluorescence images (right) of cells seeded at 30,000 cells/cm² and stained with TRITC-conjugated phalloidin. Bar, 200 μm. (F) Dot plots of total FA area (left) and number (right) as a function of cell spreading for cells plated at seeding densities of 300 (black), 3000 (green), and 30,000 (red) cells/cm². (G) Graph of cell spreading as a function of seeding density. Error bars indicate range of two independent experiments. (H) Histogram graphs of total FA area (left) and number (right) for cells plated at different seeding densities. *$p < 0.05$, **$p < 0.005$ between cells cultured at 3000 (green) or 30,000 (red) cells/cm² compared with cells at 300 cells/cm² as calculated by nonparametric median test.

formation of cell-cell contact, and fixed 24 h later for analysis (Figure 2C). Examining the total area and total number of FAs for ~100 randomly chosen cells, we observed that cells that were more spread formed more FAs regardless of the FA protein used in the analysis (Figure 2D; Supplemental Figure 1). Using this approach to determine the effects of varying cell-cell contact on FA formation and on cell spreading simultaneously, we plated cells at different densities on substrates coated with fibronectin, and measured FAs as a function of cell spreading at each seeding density (Figure 2E). At all densities and for all FA components, FA area and number formed per cell again correlated with the spreading of that cell (Figure 2F; Supplemental Figure 1). Importantly, as seeding density was increased from 300–30,000 cells/cm², cell spreading and FA formation both decreased simultaneously (Figure 2, G and H; Supplemental Figure 1). These results provide a quantitative confirmation that cell-cell contact reduces endothelial cell adhesion to, and spreading on, the extracellular matrix.

VE-Cadherin Engagement Regulates Cell Spreading and FA Formation Independently

To determine whether VE-cadherin was responsible for the effects of contact inhibition of endothelial cell adhesion and spreading, we constructed a truncated form of human VE-cadherin lacking the cytoplasmic domain responsible for interacting with β-catenin (VEΔ) that has previously been shown to act as a dominant negative (Navarro *et al.*, 1995). To promote high-efficiency expression in endothelial cells, the construct was cloned into an adenoviral expression system bicistronic with GFP (Ad-VEΔ). By Western blot analysis of Ad-VEΔ–infected cells we detected bands at 110 and 98

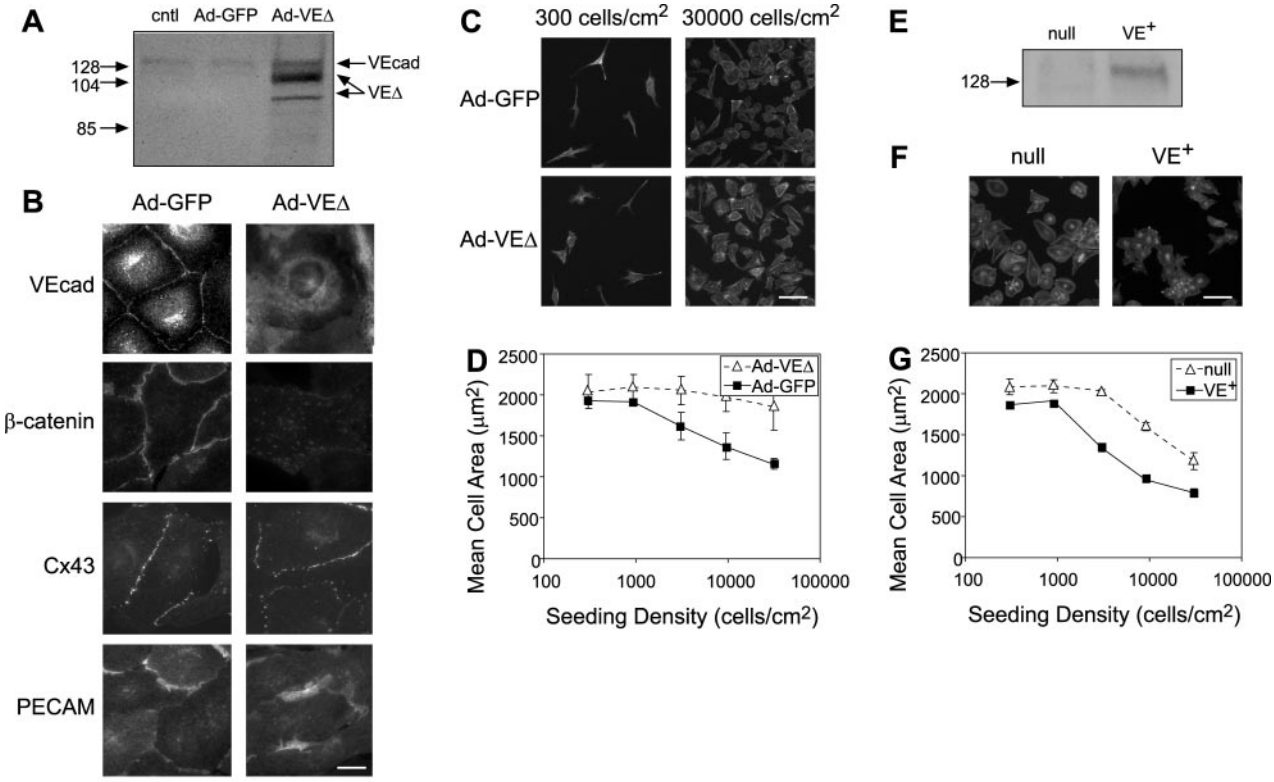

Figure 3. Density-dependent engagement of VE-cadherin decreases endothelial cell spreading. (A) Western blot for VE-cadherin for endothelial cells untreated (control) or infected with Ad-GFP or Ad-VEΔ. (B) Fluorescence images of VE-cadherin (VEcad), β-catenin, connexin 43 (Cx43), and PECAM-1 for cells infected with Ad-GFP or Ad-VEΔ. Bar, 20 μm. (C) Fluorescence images of endothelial cells infected with Ad-GFP or Ad-VEΔ and stained with TRITC-conjugated phalloidin at seeding densities of 300 and 30,000 cells/cm^2. Bar, 200 μm. (D) Graph of endothelial cell spreading as a function of seeding density for cells infected with Ad-GFP and Ad-VEΔ. (E) Western blot for VE-cadherin for A431D (null) and A431D-VE (VE$^+$) cell lysates. (F) Fluorescence images of null and VE$^+$ cells stained with TRITC-conjugated phalloidin at 9000 cells/cm^2. Bar, 200 μm. (G) Graph of cell spreading as a function of seeding density for null and VE$^+$ cells. Error bars indicate range of two independent experiments.

kDa (Figure 3A), corresponding to previously described truncated cadherin (Navarro *et al*., 1995). Infection of our cells with Ad-VEΔ resulted in a modest up-regulation of full-length VE-cadherin relative to infection with recombinant adenovirus encoding GFP alone (Ad-GFP) or uninfected control. VE-cadherin and β-catenin localized to cell-cell contacts in Ad-GFP–infected and uninfected endothelial cell controls, but not in Ad-VEΔ–infected cells (Figure 3B). The localization of other cell-cell adhesion molecules, including connexin 43 and PECAM-1, was unaffected by Ad-VEΔ. Therefore, Ad-VEΔ specifically disrupts VE-cadherin engagement in endothelial cells.

To determine whether VE-cadherin was involved in the cell-cell contact–mediated decrease in cell spreading, confluent monolayers were infected with either Ad-VEΔ or Ad-GFP control and replated at different seeding densities on substrates coated with fibronectin (Figure 3, C and D). The spreading of cells infected with Ad-GFP was similar to that of uninfected cells and decreased as seeding density increased. Disrupting VE-cadherin engagement with Ad-VEΔ abrogated the density-dependent decrease in cell spreading. Infection with Ad-VEΔ also inhibited the density-dependent decrease in focal adhesions (Supplemental Figure 2). To confirm that the engagement of VE-cadherin was responsible for decreasing cell spreading, we compared A431 carcinoma cell lines that were either cadherin-null (null) or expressed recombinant human VE-cadherin (VE$^+$) (Figure 3E). Null and VE$^+$ cells were plated at different seeding densities on substrates coated with fibronectin. As the density of cells increased, null cell spreading decreased (Figure 3, F and G). Introducing VE-cadherin caused VE$^+$ cells to grow in clusters and spread significantly less than null cells at all seeding densities. Importantly, the engagement of VE-cadherin potentiated the decrease in cell spreading with density. Together, these data suggest that VE-cadherin induces cell-cell contact-mediated inhibition of cell spreading.

Because cell-cell contact simultaneously decreased cell spreading and FAs, it was difficult to determine whether these effects were causally linked. To distinguish the effects of VE-cadherin on FAs from those on cell spreading, we introduced cell-cell contact while constraining changes in cell spreading and examined effects on FA formation. To control cell-cell contact and cell spreading, substrates were constructed containing bowtie-shaped, micrometer-sized wells with bases of fibronectin-coated glass and walls of agarose (Nelson and Chen, 2003). Cells plated on these substrates could only attach and spread in the bowtie-shaped wells. Single cells spread to fill one-half of the bowtie, whereas pairs of cells spread to each fill one-half of the bowtie and contact each other at the central constriction (Figure 4A). Cell spreading was thus controlled, and the only difference between single cells and pairs of cells was the presence of the cell-cell contact. We plated endothelial cells on bowtie-shaped substrates with wells of 750 μm^2/half,

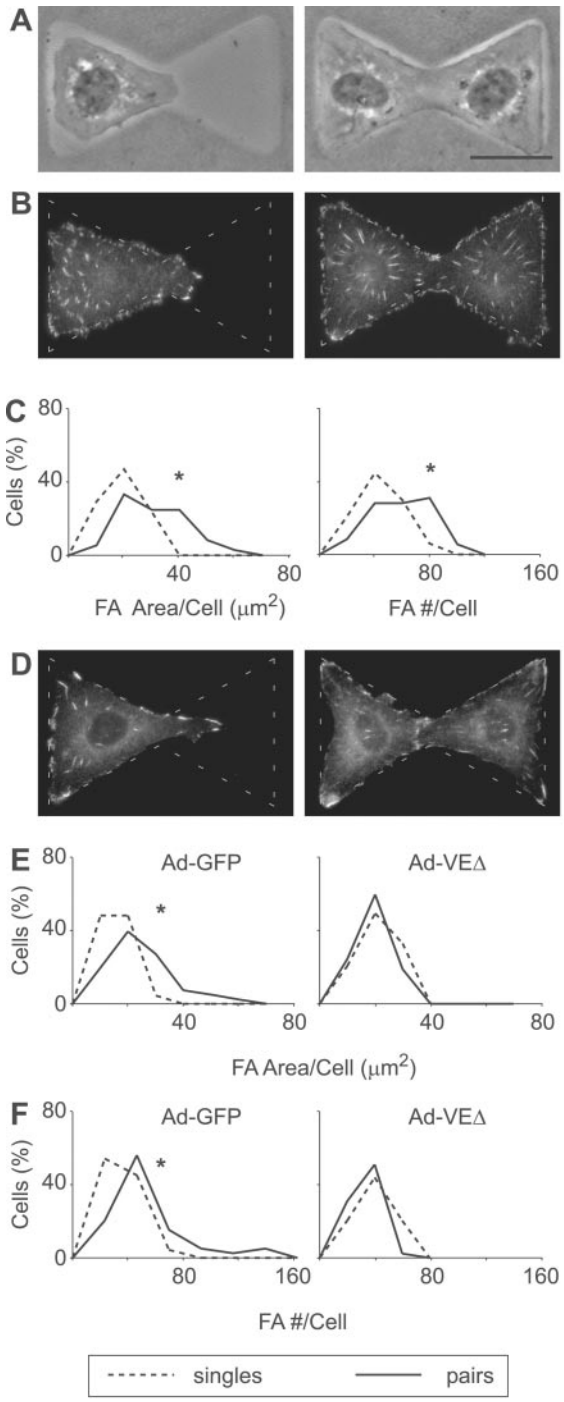

Figure 4. VE-cadherin–mediated cell-cell contact increases FA formation when spreading is controlled. (A) Phase contrast images of a single cell (left) or a pair of cells (right) cultured in the bowtie-shaped microwells. (B) Fluorescence images of a single cell (left) or a pair of cells (right) cultured in the bowtie-shaped microwells and stained for vinculin. (C) Histogram graphs of total FA area (left) and number (right) for vinculin in single cells (dotted lines) and pairs of cells (solid lines). (D) Fluorescence images of vinculin staining in a single cell (left) and a pair of cells (right) infected with Ad-VEΔ and cultured on the bowtie-shaped microwells. Histogram graphs of total area (E) and number (F) of vinculin adhesions for single cells (dotted lines) and pairs of cells (solid lines) infected with Ad-GFP or Ad-VEΔ. Dashed lines (red) indicate borders of wells in B and D. Bar, 25 μm. *$p < 0.05$ as calculated by nonparametric median test.

which maintained cell spreading constant while allowing VE-cadherin–mediated cell-cell contacts to form (Nelson and Chen, 2003), and analyzed 24 h later the total area and total number of FAs for single cells and pairs of cells (Figure 4, B and C; Supplemental Figure 3 and Table 1). Cells cultured in pairs exhibited a paradoxical increase in FA area and number over single cells. The changes in adhesions were statistically significant for all FA components examined. To determine whether VE-cadherin engagement was responsible for the contact stimulation of FA formation, we infected cells with either Ad-VEΔ or Ad-GFP control and plated them on the bowtie-shaped substrates (Figure 4, D–F). Cell-cell contact increased FA formation in Ad-GFP–infected cells. Disrupting VE-cadherin with Ad-VEΔ abrogated the increase in FA number and area seen in pairs of cells, although the pairs remained in physical contact. Thus, engagement of VE-cadherin increases FA formation when cell spreading is controlled. Together, these findings indicate that VE-cadherin-mediated disassembly of FAs depends on the contact inhibition of cell spreading and that VE-cadherin engagement can paradoxically increase FA formation via a previously masked spreading-independent mechanism.

The Effects of VE-Cadherin Are Tension Dependent

VE-cadherin engagement either decreased cell spreading and FA formation or increased FAs when changes in cell spreading were prevented. A single mechanism that might account for these paradoxical effects involves increased intracellular tension. Rho-mediated intracellular tension has been shown to decrease cell spreading (Jalink *et al*., 1994; Hirose *et al*., 1998; van Leeuwen *et al*., 1999), an effect that is supported by theoretical models (Palecek *et al*., 1999). At the same time, Rho-mediated intracellular tension has also been shown to *increase* stress fiber formation, integrin density, and FA formation in many studies (Balaban *et al*., 2001; Ballestrem *et al*., 2001).

To determine whether the VE-cadherin–mediated decrease in cell spreading required the generation of intracellular tension, we cultured cells at different densities in the presence of BDM to inhibit actin-myosin cycling (Figure 5A). Treatment with BDM inhibited the density-dependent decrease in cell spreading. Intracellular tension and myosin dynamics are mediated in part by signaling through the Rho-Rho kinase (ROCK) pathway (Amano *et al*., 2000; Bishop and Hall, 2000). To investigate whether signaling through ROCK was necessary for the VE-cadherin–mediated changes in cell spreading, we inhibited ROCK with Y-27632 in cells plated at different densities (Figure 5B). Treatment with Y-27632 shifted the baseline to a higher degree of cell spreading even at low seeding densities, consistent with inactivation of signaling through RhoA (Jalink *et al*., 1994; van Leeuwen *et al*., 1999). Inhibiting ROCK activity also abrogated the ability of cell-cell contact to decrease cell spreading. If signaling through ROCK is required for the VE-cadherin–mediated decrease in cell spreading, then blocking RhoA directly also should inhibit changes in cell spreading with cell density. To test this hypothesis, cells were infected with either a recombinant adenovirus expressing dominant negative $RhoA^{N19}$ and GFP (Ad-$RhoA^{N19}$), or Ad-GFP control (Figure 5C). Similar to the effects of treatment with Y-27632, infection with Ad-$RhoA^{N19}$ increased cell spreading relative to infection with Ad-GFP independently of seeding density. In addition, expression of $RhoA^{N19}$ inhibited the ability of cell-cell contact to decrease cell spreading. The inhibition of cytoskeletal tension did not seem to directly alter the formation of adherens junctions

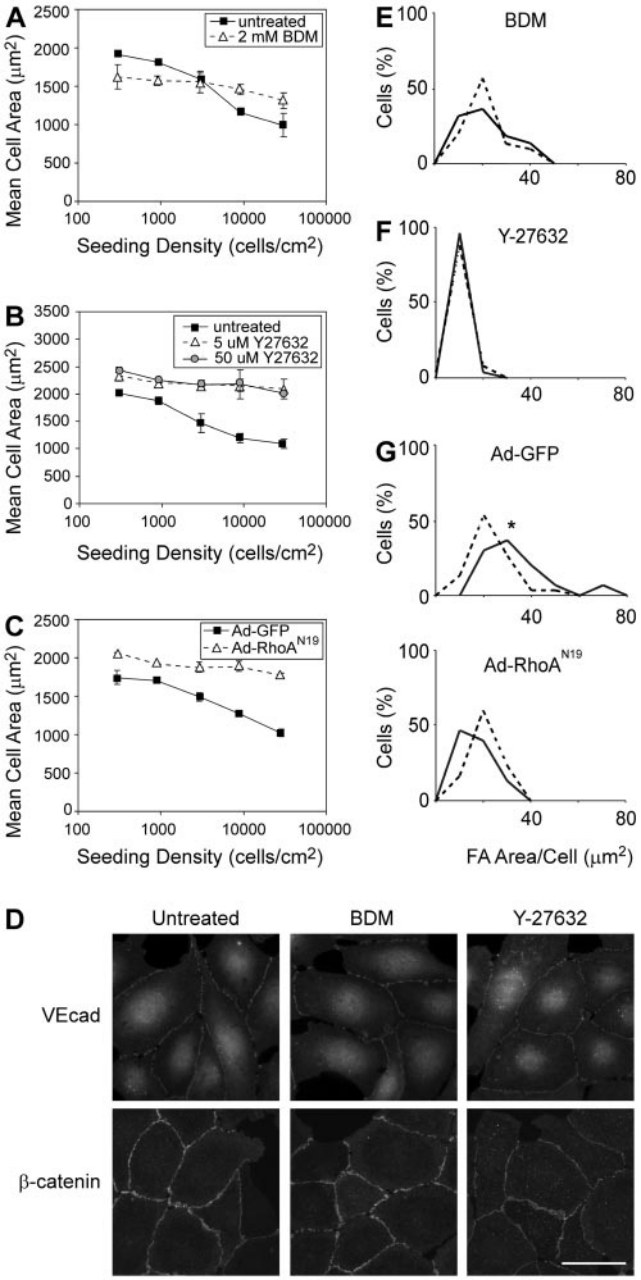

Figure 5. VE-cadherin–induced changes require RhoA-mediated signaling and tension. (A–C) Graph of endothelial cell spreading as a function of seeding density for cells treated with or without BDM (A), Y-27632 (B), or infected with Ad-RhoA^{N19} or Ad-GFP control (C). Error bars indicate range of two independent experiments. (D) Fluorescence images of untreated, 2 mM BDM-, or 50 μM Y-27632–treated endothelial cells seeded at 30,000 cells/cm^2 and stained at 24 h for VE-cadherin or β-catenin. Bar, 20 μm. (E–G) Histogram graphs of total area of vinculin adhesions for single cells (dotted lines) and pairs of cells (solid lines) treated with BDM (E), Y-27632 (F), or infected with Ad-RhoA^{N19} or Ad-GFP control (G). *$p < 0.05$ as calculated by nonparametric median test.

(Figure 5D). VE-cadherin thus inhibits cell spreading through a Rho-ROCK-tension–dependent signal.

To determine whether the VE-cadherin–mediated increase in FAs in spreading-constrained cells required the generation of intracellular tension, we cultured cells on the bowtie-shaped substrates in the presence of BDM (Figure 5E). Whereas high concentrations of BDM would typically abrogate all FA formation, treatment with low concentrations of BDM (2 mM) specifically blocked the increase in FAs in pairs of cells without altering FAs in single cells. To determine whether signaling through the Rho-ROCK pathway was necessary for the VE-cadherin–mediated increase in FAs, we inhibited ROCK or RhoA in cells plated on the bowtie-shaped substrates (Figure 5, F and G). Treatment with Y-27632 or infection with Ad-RhoA^{N19} also abrogated the increase in FAs seen in pairs of cells. Thus, the increase in FAs after VE-cadherin engagement in spreading-controlled cells also depends on the Rho-ROCK-tension signaling pathway.

The two distinct effects of VE-cadherin engagement on cell-ECM adhesions, decreased cell spreading and FA formation, and increased FAs when spreading was prevented from changing, both seem to depend on the Rho-ROCK-tension pathway.

VE-Cadherin Engagement Activates RhoA

The abrogation of both contact inhibition of cell spreading and contact stimulation of FA assembly by blocking cytoskeletal tension, Rho signaling, or ROCK activity suggested that VE-cadherin engagement might activate RhoA. To test this hypothesis, we used the previously described Rho pulldown assay to measure RhoA activity in cells with or without VE-cadherin engagement (Ren *et al*., 1999). Endothelial cells were infected with Ad-VEΔ or Ad-GFP control, resuspended, and subsequently plated at 30,000 cells/cm^2 on fibronectin-coated substrates (Figure 6, A–C). Cells were lysed at different times after plating and analyzed for GTP-bound RhoA. As has been reported for other cell types, the level of active RhoA increased when endothelial cells were stimulated with serum (Figure 6A, lanes 1 and 2) or placed in suspension (Figure 6A, lanes 3 and 4). When cells were resuspended just before plating (time 0), RhoA activity was identical in lysates from uninfected, Ad-GFP–, and Ad-VEΔ–infected cells (Figure 6A, lanes 4–6). Plating both Ad-GFP– and Ad-VEΔ–infected endothelial cells on fibronectin-coated substrates induced a transient inhibition of RhoA, similar to that observed in fibroblasts in previous reports (Ren *et al*., 1999, 2000). This initial period of RhoA inactivation was followed by a transient increase in RhoA activity that peaked at 90 min after plating. In Ad-VEΔ–infected cells, RhoA activity then steadily decreased. These results are in agreement with the biphasic regulation of RhoA by integrin-mediated adhesion and spreading on ECM reported by Ren *et al*., 1999. In Ad-GFP–infected cells, a second transient peak in RhoA activity was observed at 6 h after plating. This second peak in activity occurred soon after the localization of VE-cadherin, p120-catenin and β-catenin to cell-cell contacts, which occurred at 4–6 h after plating in Ad-GFP– but not Ad-VEΔ–infected cells (Figure 6D; Supplemental Figure 4). To confirm that VE-cadherin–mediated cell-cell adhesion was responsible for the second peak in active RhoA, we plated Ad-GFP–infected cells at a low seeding density, 9000 cells/cm^2, and repeated the RhoA activity time course (Figure 6E). Plating endothelial cells at a low density decreased cadherin engagement and elicited only the first phase of transient RhoA activation, similar to that observed in high-density Ad-VEΔ–infected cells. Therefore, the second peak in RhoA activity in high-density Ad-GFP–infected cells can be attributed specifically to the engagement of VE-cadherin at cell-cell contacts; blocking VE-cadherin engagement either by expression of the VEΔ construct or by reducing cell–cell interaction eliminated this

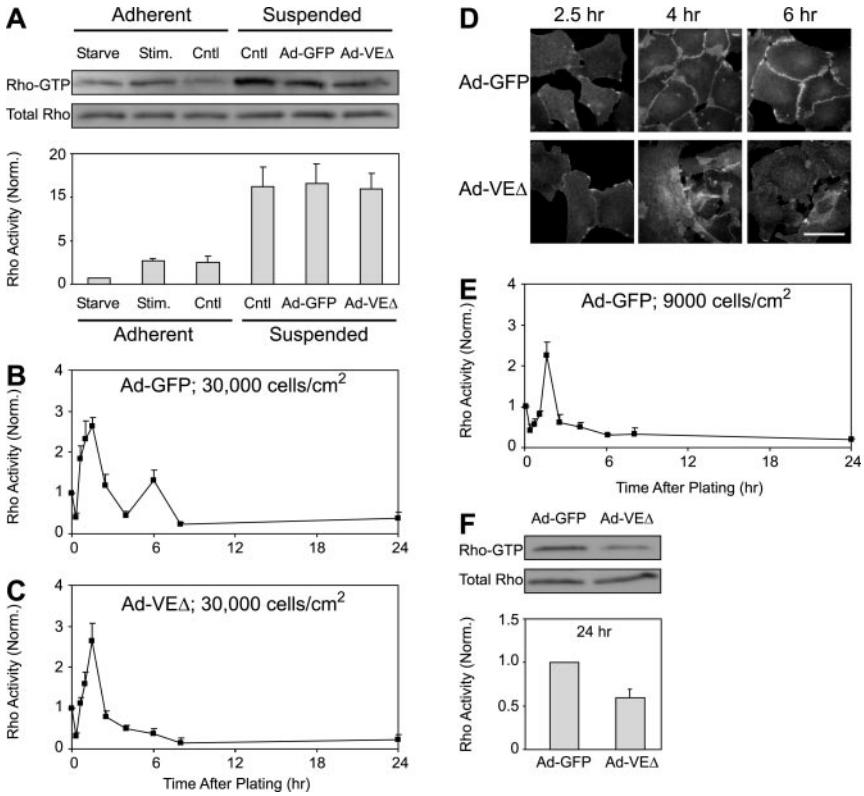

Figure 6. Engagement of VE-cadherin activates RhoA. (A) Pulldown experiments for GTP-bound RhoA in endothelial cells that were uninfected controls (cntl) or infected with Ad-GFP or Ad-VEΔ and subsequently detached and held in suspension (time 0). As a comparison, adherent monolayers that were serum starved (starve), stimulated for 5 min with media containing 5% serum (stim.), or unstarved controls (cntl) were lysed before detachment (adherent). (B, C, and E) RhoA activity in cells infected with Ad-GFP (B and E) or Ad-VEΔ (C) and replated on fibronectin-coated dishes at 30,000 cells/cm^2 (B and C) or 9000 cells/cm^2 (E). RhoA was assayed by pulldown experiments at indicated times, and values were normalized relative to time 0. (D) Fluorescence images of Ad-GFP– and Ad-VEΔ–infected cells stained for p120-catenin at different times after plating. Bar, 25 μm. (F) RhoA activity in cells infected with Ad-GFP or Ad-VEΔ, 24 h after replating at 30,000 cells/cm^2 on fibronectin-coated substrates. Data are mean ± SE from three or more experiments.

peak. At 24 h after plating, Ad-VEΔ–infected cells still had 50% less GTP-bound RhoA than did cells with normal VE-cadherin engagement (Figure 6F). Thus, the initial engagement of VE-cadherin rapidly and transiently activates RhoA, and continued engagement is responsible for its sustained activation.

DISCUSSION

It has long been thought that cadherins could modulate changes in cell structure and adhesion, possibly through direct mechanical effects as well as through biochemical signals (Shay-Salit *et al*., 2002; Vaezi *et al*., 2002). However, experimental limitations have made it difficult to describe these effects and the molecular mechanisms involved. Here, we used quantitative measures of cell spreading and FA formation to show that cell-cell contact through VE-cadherin decreases cell spreading, and consequently, disassembles FAs in endothelial cells. When cell spreading is controlled, VE-cadherin paradoxically increases FA formation. Furthermore, we show that VE-cadherin mediates both effects by activating RhoA to alter intracellular tension (Figure 7).

Ours is the first report of RhoA activation by the engagement of VE-cadherin in endothelial cells. For other cadherins, it has been reported that RhoA is stimulated by N-cadherin engagement in C2C12 myoblasts (Charrasse *et al*., 2002) and by E-cadherin engagement in keratinocytes (Calautti *et al*., 2002). However, other investigators have found that cell-cell contact through cadherins inhibits RhoA activity (Noren *et al*., 2001; Lampugnani *et al*., 2002), whereas still others detect no changes in RhoA upon cadherin engagement (Nakagawa *et al*., 2001). The differences among the results reported might be due to differences between the cadherin molecules or cell types studied, or even the specific experimental conditions used, given that RhoA activity is affected by many stimuli in the surrounding microenvironment, including growth factor concentrations and integrin ligation. The timing of the RhoA activity measurement also is critical. Dramatic, complex changes in Rho GTPase activity in response to integrin ligation have been well described (Ren *et al*., 1999). We see similarly complex effects due to cadherin engagement. Only by plating cells such that initial integrin and cadherin engagement were separated by several hours did we detect two peaks in RhoA activity after endothelial cell plating; the first was attributable to integrin binding to fibronectin, whereas the second was due to the engagement of VE-cadherin. Although RhoA activity eventually declined, the level of active RhoA was still significantly higher in cells with cadherin-mediated contacts even at 24 h, suggesting that prolonged cadherin engagement continues to affect steady-state levels of active RhoA. Thus, the timing of cadherin engagement and assaying for RhoA activity is clearly critical to the proper characterization of the

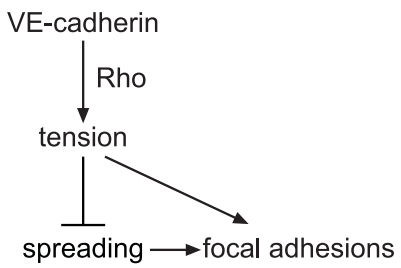

Figure 7. Schematic of proposed model. VE-cadherin activates RhoA, which increases intracellular tension, leading to a decrease in cell spreading as well as an increase in FA formation.

effects of VE-cadherin and may explain some of the differences between published results.

Although the molecular mediators responsible for cadherin-induced RhoA activation are not known, several mechanisms have been proposed (Braga, 2002; Yap and Kovacs, 2003). Although in this study we specifically block VE-cadherin engagement to abrogate signaling, engagement alone might not be sufficient for RhoA activation. The anchoring of cadherins to the actin cytoskeleton via numerous scaffolding proteins also may be required. For example, cadherins bind to and sequester p120-catenin; cytoplasmic p120-catenin inactivates RhoA, and cadherin binding is thought to inhibit this inactivation (Noren *et al*., 2000; Anastasiadis and Reynolds, 2001; Grosheva *et al*., 2001; Magie *et al*., 2002). This mechanism is consistent with the time courses of p120-catenin localization and RhoA activation in our study. Rho GTPase activity is also tightly controlled both temporally and spatially by guanine nucleotide exchange factors and GTPase-activating proteins (GAPs). It is thought that cadherins activate the Rho GTPase Rac1 by activating guanine nucleotide exchange factors and down-regulating GAPs, raising the possibility that similar mechanisms exist for the activation of RhoA (Nakagawa *et al*., 2001; Noren *et al*., 2001; Betson *et al*., 2002; Lampugnani *et al*., 2002). Elucidating the signaling pathways from cadherins to Rho GTPases will provide important clues as to how these intercellular junctions regulate cellular and multicellular organization.

Contact inhibition of cell spreading has long been noted in numerous systems (Abercrombie and Turner, 1978; Yap and Manley, 1993), but the molecular mediators have remained a matter of speculation. Our data show that the engagement of VE-cadherin and subsequent activation of the Rho-ROCK-tension pathway are responsible for this effect in endothelial cells and support prior associations of RhoA activity with inhibition of cell spreading (Jalink *et al*., 1994; Hirose *et al*., 1998; van Leeuwen *et al*., 1999). Importantly, signaling through the Rho pathway also mediates the VE-cadherin–stimulated increase in FAs when changes in cell spreading are prevented. Although it is experimentally not feasible to measure RhoA activity directly in our bowtie system, the abrogation of cadherin-induced FA assembly with Y-27632 and Ad-RhoA^{N19} demonstrates the importance of Rho signaling in this process. Like the effects on cell spreading, the Rho-mediated increase in FAs depends on changes in cytoskeletal tension, as has been described by others (Ridley *et al*., 1992; Nobes and Hall, 1995; Chrzanowska-Wodnicka and Burridge, 1996; Clark *et al*., 1998; Riveline *et al*., 2001). Because both effects are mediated by Rho, the switch in how cells respond to cadherin engagement seems not to be due to a biochemical signal, but rather it is actuated by mechanical conditions. That is, the VE-cadherin–mediated increase in contractile forces either overcomes the strength of cell adhesion and consequently changes cell shape, or reinforces FAs (Figure 7). The dependence of this balance of contractile force and adhesion strength on the local microenvironment may explain why some investigators have noted increases in FAs resulting from cell-cell contact (Lampugnani *et al*., 2002), whereas others have seen decreases (Hormia *et al*., 1985; Hodivala and Watt, 1994; Levenberg *et al*., 1998). A similar apparently paradoxical switching mechanism has been suggested in the spatial regulation of FAs during migration, in which RhoA activation near the leading edge of cells leads to FA maturation and mechanical reinforcement, whereas RhoA activation at the trailing edge causes FA disruption and tail retraction (Webb *et al*., 2002). Our studies may indicate that these two behaviors (reinforcement and disassembly) can be elicited globally in the cell, leading to generalized FA strengthening or cell retraction.

Although these data implicate VE-cadherin engagement as the principal mediator of contact-dependent alterations in cell shape and focal adhesions in endothelial cells, they cannot exclude the involvement of additional cell-cell communication pathways. Endothelial cells produce and secrete numerous growth factors, so differences between single cells and pairs of cells in the bowtie experiments and between low- and high-density cells in the density experiments also could be affected by factors other than those considered here. More directly, given the known cross talk between VE-cadherin and the VEGF receptor (Carmeliet *et al*., 1999), disrupting VE-cadherin with Ad-VEΔ might alter growth factor signaling to contribute to the observed changes. VEGF has a central role in regulating vascular permeability and angiogenesis (Ferrara *et al*., 2003), and thus an understanding of its ability to regulate the cadherin- and integrin-based adhesion systems is an important avenue of study. Nonetheless, our data implicate a critical role for VE-cadherin signaling through RhoA to affect cell shape and focal adhesions, and they support the growing body of evidence suggesting that cell-cell and cell-matrix adhesion are mechanically coupled in endothelial cells (Davies *et al*., 1997; Dudek and Garcia, 2001). Many inflammatory agents that are known to induce permeability by disrupting junctional VE-cadherin, including peroxide and histamine, may mediate part of their effects indirectly through the cadherin-mediated changes in cell-matrix adhesion (Alexander and Elrod, 2002). Thus, this VE-cadherin-Rho-FA cross talk may play an active role in the evolution of a variety of physiological and pathological conditions involved in the disruption and resealing of the endothelium.

The changes in cell structure elicited by VE-cadherin engagement are also consistent with several multicellular transformations apparent during morphogenesis. The increase in cell spreading resulting from disrupting cadherin-mediated adhesion reported here may constitute the early changes observed at the initiation of coordinated movements of sheets of cells after a scratch wound (Etienne-Manneville and Hall, 2002), or the increased cell spreading and motility after reduced cadherin function seen during epithelial-mesenchymal transition in other cell types (Savagner, 2001). Conversely, cadherins are also important for cellular compaction and mesenchymal-epithelial transitions during tissue morphogenesis and development (Gumbiner, 1996; Etienne-Manneville and Hall, 2002). Our work suggests that during their physical rearrangements relative to one another, cells might use the engagement of cadherins as a switch to initiate contraction-dependent morphogenetic changes or as a checkpoint to ensure the proper positioning of cells.

These data support the growing body of evidence that cells use both cadherins and integrins cooperatively to probe their physical surroundings (Juliano, 2002). Like integrins, cadherins now seem to broadly engage many signaling systems, including the RhoA pathway described here, as well as the previously reported Rac, Erk, PKC, and Akt pathways (Lewis *et al*., 1994; Carmeliet *et al*., 1999; Pece and Gutkind, 2000). Thus, although numerous examples of cross talk in cadherin and integrin signaling have been suggested in the literature (Zhu and Watt, 1996; Arregui *et al*., 2000), our findings here indicate that cadherin-integrin cross talk largely depends on the ability of cadherins to profoundly affect cell mechanics. In sum, the interplay of mechanical and biochemical signals that orchestrate the dynamic physical linkages between cell-cell adhesion, cell-ECM adhesion,

and cell mechanics demonstrated here constitute early hints of the mechanisms by which cells can coordinate mechanically during the complex process of morphogenesis.

ACKNOWLEDGMENTS

We thank M. Jaggi and K. Johnson for generously providing the A431 cell lines; S. Shaw and F. Luscinskas for providing the VE-cadherin cDNA; M. Philips and P. Burbelo for providing RhoA constructs; and S. Craig, E. Dejana, J. Garcia, L. Romer, and M. Schwartz for helpful discussions. This work was supported in part by National Heart, Lung, and Blood Institute (HL 073305), National Institute of Biomedical Imaging and Bioengineering (EB 00262), the Whitaker Foundation, and the Defense Advanced Research Projects Agency. C.M.N. and J.L.T acknowledge financial support from the Whitaker Foundation.

REFERENCES

Abercrombie, M., and Turner, A.A. (1978). Contract reactions influencing cell locomotion of a mouse sarcoma in culture. Med. Biol. *56*, 299–303.

Alexander, J.S., and Elrod, J.W. (2002). Extracellular matrix, junctional integrity and matrix metalloproteinase interactions in endothelial permeability regulation. J. Anat. *200*, 561–574.

Amano, M., Fukata, Y., and Kaibuchi, K. (2000). Regulation and functions of Rho-associated kinase. Exp. Cell Res. *261*, 44–51.

Anastasiadis, P.Z., and Reynolds, A.B. (2001). Regulation of Rho GTPases by p120-catenin. Curr. Opin. Cell Biol. *13*, 604–610.

Arregui, C., Pathre, P., Lilien, J., and Balsamo, J. (2000). The nonreceptor tyrosine kinase fer mediates cross-talk between N-cadherin and beta1-integrins. J. Cell Biol. *149*, 1263–1274.

Assoian, R.K., and Schwartz, M.A. (2001). Coordinate signaling by integrins and receptor tyrosine kinases in the regulation of G1 phase cell-cycle progression. Curr. Opin. Genet. Dev. *11*, 48–53.

Balaban, N.Q., *et al*. (2001). Force and focal adhesion assembly: a close relationship studied using elastomeric micropatterned substrates. Nat. Cell Biol. *3*, 466–472.

Ballestrem, C., Hinz, B., Imhof, B.A., and Wehrle-Haller, B. (2001). Marching at the front and dragging behind: differential alphavbeta3-integrin turnover regulates focal adhesion behavior. J. Cell Biol. *155*, 1319–1332.

Betson, M., Lozano, E., Zhang, J., and Braga, V.M.M. (2002). Rac activation upon cell-cell contact formation is dependent on signaling from the epidermal growth factor receptor. J. Biol. Chem. *277*, 36962–36969.

Bishop, A.L., and Hall, A. (2000). Rho GTPases and their effector proteins. Biochem. J. *348*, 241–255.

Braga, V.M. (2002). Cell-cell adhesion and signalling. Curr. Opin. Cell Biol. *14*, 546–556.

Calautti, E., Grossi, M., Mammucari, C., Aoyama, Y., Pirro, M., Ono, Y., Li, J., and Dotto, G.P. (2002). Fyn tyrosine kinase is a downstream mediator of Rho/PRK2 function in keratinocyte cell-cell adhesion. J. Cell Biol. *156*, 137–148.

Carmeliet, P., *et al*. (1999). Targeted deficiency or cytosolic truncation of the VE-cadherin gene in mice impairs VEGF-mediated endothelial survival and angiogenesis. Cell *98*, 147–157.

Charrasse, S., Meriane, M., Comunale, F., Blangy, A., and Gauthier-Rouviere, C. (2002). N-cadherin-dependent cell-cell contact regulates Rho GTPases and beta-catenin localization in mouse C2C12 myoblasts. J. Cell Biol. *158*, 953–965.

Chen, C.S., Alonso, J.L., Ostuni, E., Whitesides, G.M., and Ingber, D.E. (2003). Cell shape provides global control of focal adhesion assembly. Biochem. Biophys. Res. Commun. *307*, 355–361.

Chrzanowska-Wodnicka, M., and Burridge, K. (1996). Rho-stimulated contractility drives the formation of stress fibers and focal adhesions. J. Cell Biol. *133*, 1403–1415.

Clark, E.A., King, W.G., Brugge, J.S., Symons, M., and Hynes, R.O. (1998). Integrin-mediated signals regulated by members of the Rho family of GTPases. J. Cell Biol. *142*, 573–586.

Davies, P.F., *et al*. (1997). Spatial relationships in early signaling events of flow-mediated endothelial mechanotransduction. Annu. Rev. Physiol. *59*, 527–549.

Dejana, E., Bazzoni, G., and Lampugnani, M.-G. (1999). Vascular endothelial (VE)-cadherin: only an intercellular glue? Exp. Cell Res. *252*, 13–19.

Dudek, S.M., and Garcia, J.G. (2001). Cytoskeletal regulation of pulmonary vascular permeability. J. Appl. Physiol. *91*, 1487–1500.

Etienne-Manneville, S., and Hall, A. (2002). Rho GTPases in cell biology. Nature *420*, 629–635.

Ferrara, N., Gerber, H.P., and LeCouter, J. (2003). The biology of VEGF and its receptors. Nat. Med. *9*, 669–676.

Geiger, B., and Bershadsky, A. (2001). Assembly and mechanosensory function of focal contacts. Curr. Opin. Cell Biol. *13*, 584–592.

Geiger, B., and Bershadsky, A. (2002). Exploring the neighborhood: adhesion-coupled cell mechanosensors. Cell *110*, 139–142.

Grosheva, I., Shtutman, M., Elbaum, M., and Bershadsky, A.D. (2001). p120 catenin affects cell motility via modulation of activity of Rho-family GTPases: a link between cell-cell contact formation and regulation of cell locomotion. J. Cell Sci. *114*, 695–707.

Gumbiner, B.M. (1996). Cell adhesion: the molecular basis of tissue architecture and morphogenesis. Cell *84*, 345–357.

Hirose, M., Ishizaki, T., Watanabe, N., Uehata, M., Kranenburg, O., Moolenaar, W.H., Matsamura, F., Maekawa, M., Bito, H., and Narumiya, S. (1998). Molecular dissection of the Rho-associated protein kinase (p160ROCK)-regulated neurite remodeling in neuroblastoma N1E-115 cells. J. Cell Biol. *141*, 1625–1636.

Hodivala, K.J., and Watt, F.M. (1994). Evidence that cadherins play a role in the downregulation of integrin expression that occurs during keratinocyte terminal differentiation. J. Cell Biol. *124*, 589–600.

Hood, J.D., and Cheresh, D.A. (2002). Role of integrins in cell invasion and migration. Nat. Rev. Cancer *2*, 91–100.

Hormia, M., Badley, R.A., Lehto, V.P., and Virtanen, I. (1985). Actomyosin organization in stationary and migrating sheets of cultured human endothelial cells. Exp. Cell Res. *157*, 116–126.

Jalink, K., van Corven, E.J., Hengeveld, T., Morii, N., Narumiya, S., and Moolenaar, W.H. (1994). Inhibition of lysophosphatidate- and thrombin-induced neurite retraction and neuronal cell rounding by ADP ribosylation of the small GTP-binding protein Rho. J. Cell Biol. *126*, 801–810.

Juliano, R.L. (2002). Signal transduction by cell adhesion receptors and the cytoskeleton: functions of integrins, cadherins, selectins, and immunoglobulin-superfamily members. Annu. Rev. Pharmacol. Toxicol. *42*, 283–323.

Ko, K.S., Arora, P.D., and McCulloch, C.A. (2001). Cadherins mediate intercellular mechanical signaling in fibroblasts by activation of stretch-sensitive calcium-permeable channels. J. Biol. Chem. *276*, 35967–35977.

Kouklis, P., Konstantoulaki, M., and Malik, A.B. (2003). VE-cadherin-induced Cdc42 signaling regulates formation of membrane protrusions in endothelial cells. J. Biol. Chem. *278*, 16230–16236.

Lampugnani, M.-G., Zanetti, A., Breviario, F., Balconi, G., Orsenigo, F., Corada, M., Spagnuolo, R., Betson, M., Braga, V., and Dejana, E. (2002). VE-cadherin regulates endothelial actin activating Rac and increasing membrane association of Tiam. Mol. Biol. Cell *13*, 1175–1189.

Levenberg, S., Katz, B.-Z., Yamada, K.M., and Geiger, B. (1998). Long-range and selective autoregulation of cell-cell or cell-matrix adhesions by cadherin or integrin ligands. J. Cell Sci. *111*, 347–357.

Lewis, J.E., Jensen, P.J., Johnson, K.R., and Wheelock, M.J. (1994). E-cadherin mediates adherens junction organization through protein kinase C. J. Cell Sci. *107*, 3615–3621.

Magie, C.R., Pinto-Santini, D., and Parkhurst, S.M. (2002). Rho1 interacts with p120ctn and alpha-catenin, and regulates cadherin-based adherens junction components in *Drosophila*. Development *129*, 3771–3782.

Nakagawa, M., Fukata, M., Yamaga, M., Itoh, N., and Kaibuchi, K. (2001). Recruitment and activation of Rac1 by the formation of E-cadherin-mediated cell-cell adhesion sites. J. Cell Sci. *114*, 1829–1838.

Navarro, P., Caveda, L., Breviario, F., Mandoteanu, I., Lampugnani, M.-G., and Dejana, E. (1995). Catenin-dependent and -independent functions of vascular endothelial cadherin. J. Biol. Chem. *270*, 30965–30972.

Nelson, C.M., and Chen, C.S. (2002). Cell-cell signaling by direct contact increases cell proliferation via a PI3K-dependent mechanism. FEBS Lett. *514*, 238–242.

Nelson, C.M., and Chen, C.S. (2003). VE-cadherin simultaneously stimulates and inhibits cell proliferation by altering cytoskeletal structure and tension. J. Cell Sci. *116*, 3571–3581.

Nobes, C.D., and Hall, A. (1995). Rho, Rac and Cdc42 GTPases regulate the assembly of multimolecular focal complexes associated with actin stress fibers, lamellipodia, and filopodia. Cell *81*, 53–62.

Noren, N.K., Liu, B.P., Burridge, K., and Kreft, B. (2000). p120 catenin regulates the actin cytoskeleton via rho family GTPases. J. Cell Biol. *150*, 567–579.

Noren, N.K., Niessen, C.M., Gumbiner, B.M., and Burridge, K. (2001). Cadherin engagement regulates Rho family GTPases. J. Biol. Chem. *276*, 33305–33308.

Palecek, S.P., Horwitz, A.F., and Lauffenburger, D.A. (1999). Kinetic model for integrin-mediated adhesion release during cell migration. Ann. Biomed. Eng. *27*, 219–235.

Pece, S., and Gutkind, A.S. (2000). Signaling from E-cadherins to the MAPK pathway by the recruitment and activation of epidermal growth factor receptors upon cell-cell contact formation. J. Biol. Chem. *275*, 41227–41233.

Plopper, G., and Ingber, D.E. (1993). Rapid induction and isolation of focal adhesion complexes. Biochem. Biophys. Res. Commun. *193*, 571–578.

Pokutta, S., and Weis, W.I. (2002). The cytoplasmic face of cell contact sites. Curr. Opin. Sruct. Biol. *12*, 255–262.

Putnam, A.J., Cunningham, J.J., Pillemer, B.B., and Mooney, D.J. (2003). External mechanical strain regulates membrane targeting of Rho GTPases by controlling microtubule assembly. Am. J. Physiol.. *284*, C627–C639.

Ren, X.D., Kiosses, W.B., and Schwartz, M.A. (1999). Regulation of the small GTP-binding protein Rho by cell adhesion and the cytoskeleton. EMBO J. *18*, 578–585.

Ren, X.D., Kiosses, W.B., Sieg, D.J., Otey, C.A., Schlaepfer, D.D., and Schwartz, M.A. (2000). Focal adhesion kinase suppresses Rho activity to promote focal adhesion turnover. J. Cell Sci. *113*, 3673–3678.

Ridley, A.J., Paterson, H.F., Johnston, C.L., Diekmann, D., and Hall, A. (1992). The small GTP-binding protein Rac regulates growth factor-induced membrane ruffling. Cell *70*, 401–410.

Riveline, D., Zamir, E., Balaban, N.Q., Schwartz, U.S., Ishizaki, T., Narumiya, S., Kam, Z., Geiger, B., and Bershadsky, A. (2001). Focal contacts as mechanosensors: externally applied local force induces growth of focal contacts by an mDia1-dependent and ROCK-independent mechanism. J. Cell Biol. *153*, 1175–1183.

Ryan, P.L., Foty, R.A., Kohn, J., and Steinberg, M.S. (2001). Tissue spreading on implantable substrates is a competitive outcome of cell-cell vs. cell-substratum adhesivity. Proc. Natl. Acad. Sci. USA *98*, 4323–4327.

Savagner, P. (2001). Leaving the neighborhood: molecular mechanisms involved during epithelial-mesenchymal transition. Bioessays *23*, 912–923.

Shay-Salit, A., Shushy, M., Wolfovitz, E., Yahav, H., Breviario, F., Dejana, E., and Resnick, N. (2002). VEGF receptor 2 and the adherens junction as a mechanical transducer in vascular endothelial cells. Proc. Natl. Acad. Sci. USA *99*, 9462–9467.

Stupack, D.G., and Cheresh, D.A. (2002). Get a ligand, get a life: integrins, signaling and cell survival. J. Cell Sci. *115*, 3729–3738.

Vaezi, A., Bauer, C., Vasioukhin, V., and Fuchs, E. (2002). Actin cable dynamics and Rho/Rock orchestrate a polarized cytoskeletal architecture in the early steps of assembling a stratified epithelium. Dev. Cell *3*, 367–381.

van Leeuwen, F.N., van Delft, S., Kain, H.E., van der Kammen, R.A., and Collard, J.G. (1999). Rac regulates phosphorylation of the myosin-II heavy chain, actinomyosin disassembly and cell spreading. Nat. Cell Biol. *1*, 242–248.

Vestweber, D. (2000). Molecular mechanisms that control endothelial cell contacts. J. Pathol. *190*, 281–291.

Webb, D.J., Parsons, J.T., and Horwitz, A.F. (2002). Adhesion assembly, disassembly and turnover in migrating cells – over and over and over again. Nat. Cell Biol. *4*, E97–E100.

Yap, A.S., and Kovacs, E.M. (2003). Direct cadherin-activated cell signaling: a view from the plasma membrane. J. Cell Biol. *160*, 11–16.

Yap, A.S., and Manley, S.W. (1993). Contact inhibition of cell spreading: a mechanism for the maintenance of thyroid cell aggregation in vitro. Exp. Cell Res. *208*, 121–127.

Zhu, A.J., and Watt, F.M. (1996). Expression of a dominant negative cadherin mutant inhibits proliferation and stimulates terminal differentiation of human epidermal keratinocytes. J. Cell Sci. *109*, 3013–3023.